

Microbubbles as a Skin Friction Reduction Device -A Midterm Review of the Research

Hiroharu KATO
Department of Mechanical Engineering,
Toyo University

and

Yoshiaki KODAMA
Center for Smart Control of Turbulence
National Maritime Research Institute

Abstract

First, we introduce the research works recently conducted by the SR 239 Research Committee: (1) a full-scale microbubble experiment on the Seiun-Maru, and (2) an air-sheet experiment. We discuss possible mechanisms of frictional resistance reduction by microbubbles. When the size of microbubbles is of the order of 0.1mm, the viscosity increase caused by microbubbles seems to be the governing mechanism. When the size of microbubbles is much larger than 0.1mm, the homogenization effect by microbubbles may be the governing mechanism.

1. Introduction

The present joint research work started 4 years ago in 1999. It is both important and instructive to review the 4-year development of experimental as well as theoretical research on microbubbles as a skin friction reduction device.

During that period, some of the members also engaged in another research project on microbubbles, which was performed by the SR 239 Research Committee of the Japan Shipbuilding Research Association. The purpose of the project was to find practical methods for skin friction reduction of ships. The research was conducted for 4 years, from April 1998 to March 2002, with the participation of many major Japanese shipbuilding companies, universities and the National Maritime Research Institute. We introduce the results on microbubbles, focusing on the full-scale experiment on the Seiun-Maru (Kodama et al. (2002b), Nagamatsu et al. (2002)), and air sheet. We then proceed to discuss the skin friction reduction mechanisms of microbubbles, based on the findings already obtained and the questions to be answered through future research.

2. The SR239 Full-Scale Microbubble Experiment

Experimental results

Numerous laboratory experiments have shown that microbubbles are very effective in skin friction reduction. However, no full-scale experiment had been conducted until the SR 239 Research Committee performed a full-scale experiment using the Seiun-Maru in September 2001. Since the practical application of microbubbles to ships is the final goal of the current research project, the experiment is described here in detail, based on the published reports already referenced.

The Seiun-Maru is a training ship that belongs to the National Institute for Sea Training, Japan (Fig. 1). The particulars are shown in Table 1. Three horizontal air duct branches were installed on each side (port and starboard) of the Seiun-Maru for air ejection, as shown in Fig. 2. Six sets of mobile air compressors on the deck supplied air to the ducts, totaling 110m³/min (nominal) at the

maximum compressor power. The air was ejected into the boundary layer on the hull surface through small holes drilled in the horizontal part of the branch ducts.

Figure 3 shows the airflow along the hull predicted using CFD. The air bubble flow, shown in red, goes down to the bottom before the middle part at around SS 7 (Square Station 7) and comes up again in the stern part at around SS 3. According to the calculation the air bubbles cover the hull surface well. The calculation was one-way coupling, which took into account the effect of buoyancy and drag of individual bubbles.



Fig. 1 Seiuin-Maru

Table 1 Particulars of the Seiuin-Maru

Length overall	116.0m
Lpp	105.0m
Breadth	17.9m
Depth	10.8m
Draft	6.3m
Gross tonnage	5884t
Displacement	6325.4t
Speed (Max)	21.0 knot
Max. Cont. Rating	10500 PS



Fig. 2 Air ejection ducts

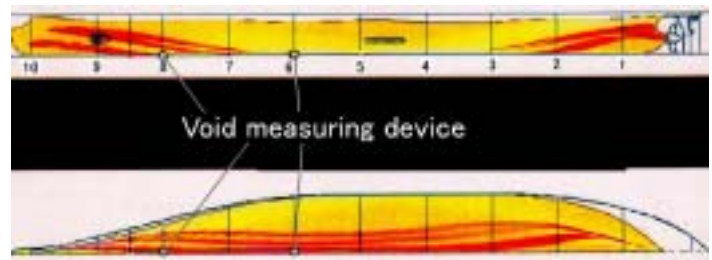


Fig. 3 Calculated airflow along the hull (Kato et al., 2003)

Seven sets of shearing stress sensors and two sets of void measuring devices were installed on the fore part of the hull surface, on the port side, based on the predicted air bubble path. The shearing stress sensors measured the shearing force acting on the sensor plate of 200mm×200mm. The void measuring device captured images of microbubbles through its side window, and analyzed the image using an image processing software to get the bubble number and size distributions (Kato et al. (2003)).

The full-scale experiment was carried out for three days in the Pacific Ocean, off Tokyo Bay. The weather was fine and the sea was calm throughout. The wave height was less than 1m. A total of 50 runs were performed with and without air ejection at the ship speed of 14-21knots. At each run the propeller rotation was kept constant, and the ship speed at air ejection and non-ejection cases was measured using GPS. In order to cancel out the wind and tide effects the measured values in the two runs in opposite directions within a short period of time were averaged. Since the measurement of ship drag was impossible, we measured the thrust of the propeller instead and estimated the drag by assuming that the propeller-hull interaction remained unchanged.

Contrary to our original expectation, the ship speed was reduced upon bubble ejection under many experimental conditions. Figure 4 shows the results, in which the bubbles were ejected from both the upper and lower ejection ducts, with the maximum compressor power (ALL MAX) or one

half of the maximum power (ALL 1/2 MAX). It is seen that all the symbols corresponding to the bubble ejection cases lie to the left of the non-bubble symbols, and when compared at a constant speed, the non-bubble curve is located at the bottom of the three, which means that thrust increase was needed in the bubble cases in order to maintain the same speed. But fortunately there were only a few cases in which the reduction of ship drag (propeller thrust) was obtained. Figure 5 shows the reduction of the propeller thrust at about 13.5 knots. The solid triangle shows the case in which the bubbles were ejected from both the upper and lower ejection ducts at 1/4 compressor power (28m³/min) (All 1/4 MAX). The open triangle shows the case in which the bubbles were ejected only from the upper branch duct at the maximum compressor power (Upper MAX), but the amount of air was 38 m³ (max of the ejection branch). It should be noted that the amount of air was much less than the total capacity of all the air compressors. The open square shows the lower branch, the maximum compressor power case (Lower MAX). Broken curves show the speed squared relation passing through each symbol, correspond to the speed-thrust curves.

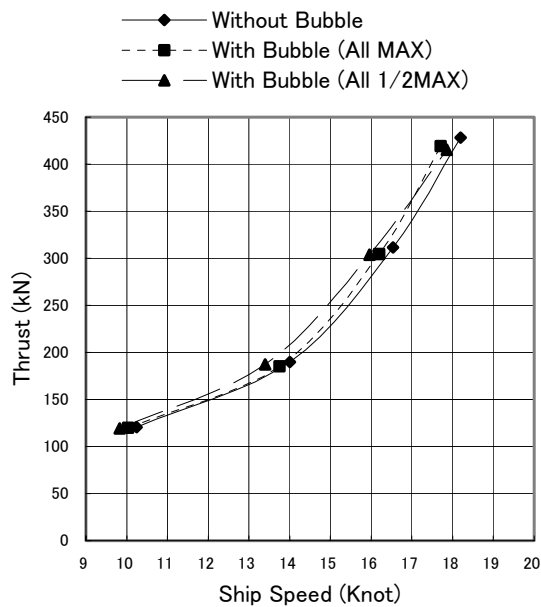


Fig. 4 Thrust increase by microbubbles (Nagamatsu et a. 2002)

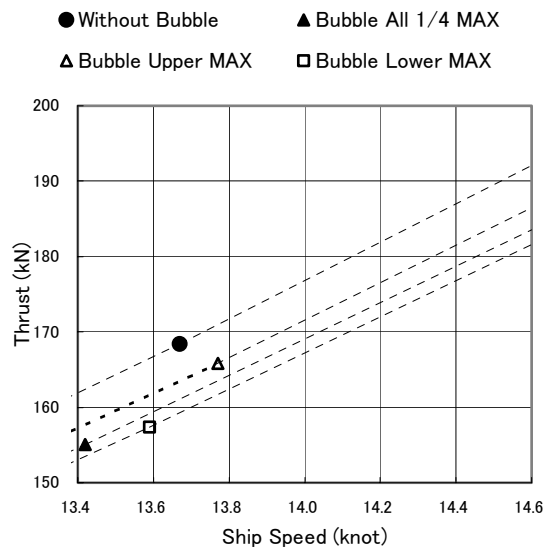


Fig. 5 Thrust reduction by microbubbles (Nagamatsu et al., 2002)

Figure 6 shows the local shearing force measured by the shearing stress sensors. Both sensors No. 3 and No. 4 were installed at the same SS 8, with No. 4 at a position (2.42m from the base line) higher than No.3. The shearing stress measured with No. 4 was reduced with bubbles in almost the entire speed range, whereas that with No.3 showed the opposite results, that is, the shearing stress increased with air bubbles.

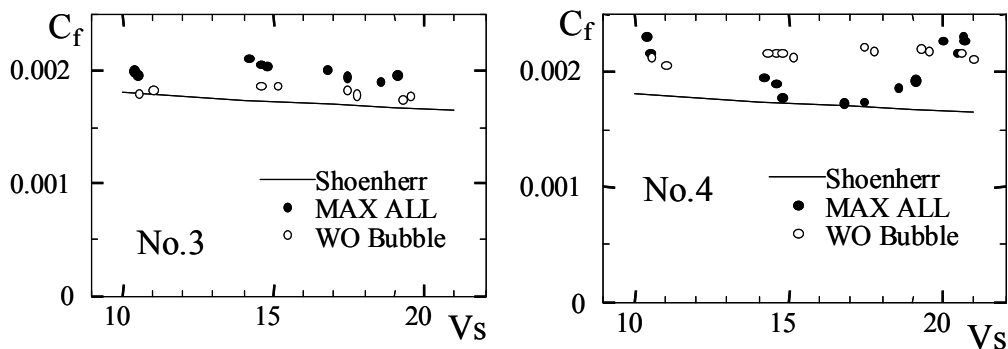


Fig. 6 Local shearing force on hull surface (Nagamatsu et al., 2002)

Figure 7 shows the void distribution across the boundary layer on the bottom surface at SS 6, measured by a void sensor. The peak location in the distribution is between 5 and 10mm from the surface, which means that there is a gap between the bubble layer and the surface. There was no reduction of the skin friction measured using the shear stress sensor No.6 positioned only 0.76m away from the void sensor. The void distribution in the boundary layer of a flat plate measured in the towing tank of the NMRI is shown in Figure 8. Two types of air ejection ducts, designed respectively by Mitsubishi and by the NMRI, were tested. The peak of the void distribution was very close to the bottom surface in the both cases. There was a 15-18% reduction of skin friction by microbubbles (Kodama et al. (2002b), Kato et al. (2003)). Therefore it is suspected that, in the full scale experiment, the skin friction did not reduce because there was a gap between the bubble layer and the hull surface and the hull surface.

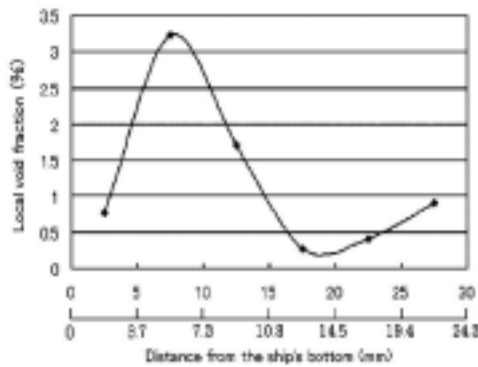


Fig. 7 Void distribution in the boundary layer of Seiun-Maru (Kato, et al., 2003)

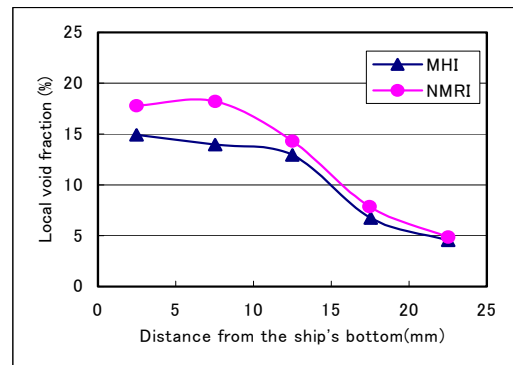


Fig. 8 Void distribution in the boundary layer of a flat plate (Kato, et al., 2003)

Discussions

It is important to discuss some issues possibly related to the fact that the drag and necessary engine horsepower increased in many cases. The first issue is the buoyancy effect. It is suspected that the ejected air bubbles did not stay in the inner region of the boundary layer well. The observation of bubble ejection using an underwater TV camera showed that the ejected bubbles did not spread thinly over the hull but flowed like chimney smoke. Figure 7 shows that the bubbles were slightly away from the hull surface. Also it is interesting to note that the air ejection rate was not maximum when the best result was obtained, as mentioned above. These facts suggest that the buoyancy effect of a mass of bubbles is much greater than that of a single bubble in the calculation, and acted to move the bubbles away from the hull surface. This hypothesis is further supported by the fact that the actual bubble flow trajectory deviated significantly upward from the prediction. Although a preliminary test of the air ejection duct was performed in the towing tank of the NMRI, the buoyancy effect could not be tested properly, because the air ejector was set on the horizontal flat plate.

The second issue is the reduction of the propeller performance. The efficiency of the propeller was reduced 3-6 % by the air ejection. The propeller thrust was also reduced. We anticipated the thrust reduction, because the effective density of flow into the propeller reduces by air bubbles, but this effect was larger than predicted. In the experiment, we also observed the reduction of efficiency. This might have been caused by the decrease of the lift-drag ratio due to air bubbles.

By considering all those results, we can conclude that the location of bubbles in the boundary layer is extremely important for the skin friction reduction. In other words microbubbles are very effective in reducing skin friction, if they can be concentrated in the inner region of the boundary layer, close the wall.

3. The SR239 Air Sheet Experiment for Skin Friction Reduction

Another interesting research target of the SR 239 project was an air sheet (air film) as a frictional resistance reduction device (Shimoyama, 2002). The project group performed an experiment with an air sheet under a horizontal flat plate in a cavitation tunnel. Figure 9 shows a sketch of the air sheet behavior. The air sheet formed for a short distance from the outlet, and then disintegrated into bubbles further downstream.

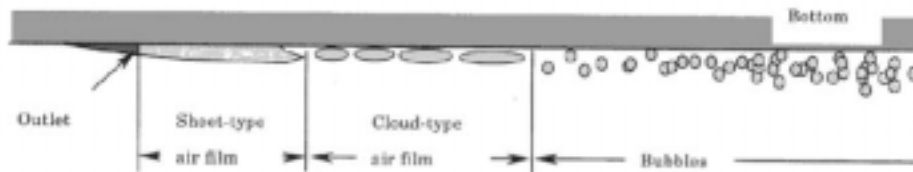


Fig. 9 Air behavior downstream of air sheet (Shimoyama, 2002)

Figure 10 shows a photograph taken in the cavitation tunnel. The area of the air sheet decreased with water velocity.

They also performed air sheet experiments using a model ship ($L=7\text{m}$) and a long flat-bottom model ship ($L=16\text{m}$). Substantial drag reduction was obtained in the two cases; the drag reduction of the former model ship ($L=7\text{m}$) was 10~15% and that of the long model ship ($L=16\text{m}$) was 30% at 4 m/s and 20% at 7 m/s.

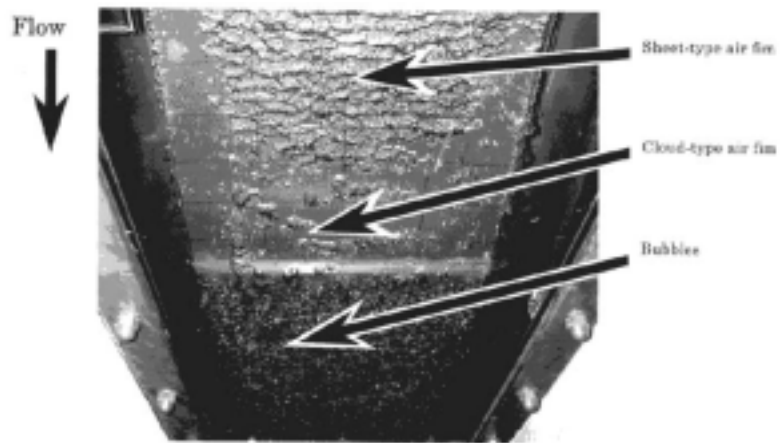


Fig. 10 Photograph of the air sheet in a cavitation tunnel (Shimoyama, 2002)

The advantage of using an air sheet is the larger reduction of frictional resistance than microbubbles. However, the formation and preservation of the air sheet is extremely difficult, particularly at a higher speed. The air sheet length in the flat plate experiment was only about 20cm at 7 m/s. When they increased the air ejection rate and increased the air sheet thickness, waves were generated at the air-water interface, which caused drag increase.

Their interesting finding was substantial reduction of the frictional resistance in the region covered by air bubbles that formed downstream of the air sheet. This suggests the simultaneous use of air sheet and microbubbles from a single air source, for better skin friction reduction performance.

4. Mechanism of Skin Friction Reduction by Microbubbles

Here, we would like to discuss our present knowledge of microbubbles by listing the related findings and questions, in order to understand the mechanism of drag reduction by microbubbles.

Findings:

1. When microbubbles are present in the turbulent boundary layer, the wall frictional resistance is reduced. This reduction can also be observed in duct flow. The reduction rate is more than 50% under optimum conditions (Bogdevich et al. (1977), Madavan et al. (1985A), Kato et al. (1995)).

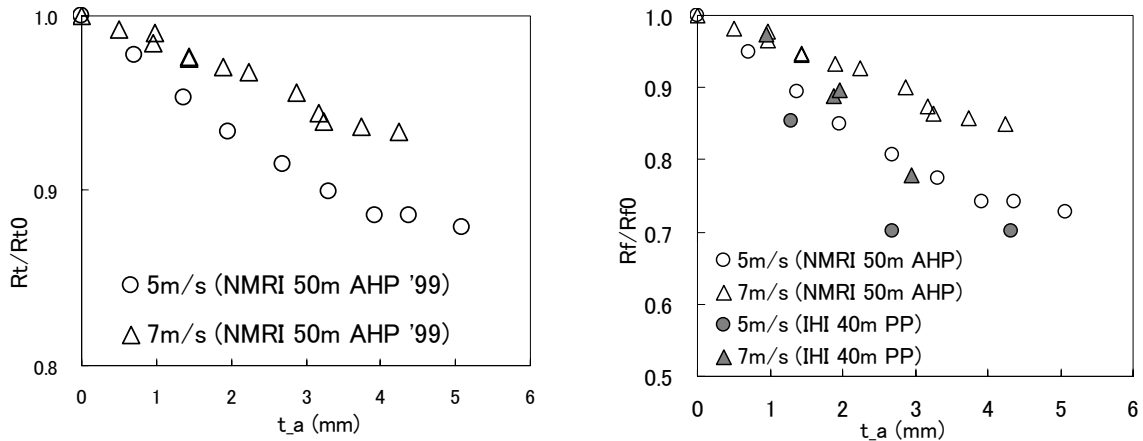
2. A few experiments showed much more than 50% frictional resistance reduction, but such large reduction was observed only near the region of microbubble ejection. To the contrary, the frictional resistance reduction can be preserved 50m downstream of the microbubble ejection point (Watanabe et al. (1999), Takahashi et al. (2001), Kodama (2002)).
3. If the diameter of microbubbles is in the range between 0.4 and 2.2mm, the bubble size does not affect the reduction of frictional resistance (Moriguchi and Kato (2002)). The void ratio, probably the void ratio in the inner region of the boundary layer, is important, and governs the mechanism (Guin et al. (1996)).
4. The orientation of the wall also affects drag reduction. The wall-on-top condition gives the largest reduction. This can be easily explained by the fact that the bubble buoyancy favorably affects on the reduction (Kato et al. (1995)).

Figure 11 shows the results of the microbubble experiment using a 50m long flat ship at NMRI (Kodama et al 2002a). Air was ejected through an Array of Holes Plate (AHP), a plate with many 1mm diameter holes drilled at 3 to 5mm pitch. Figure 11(a) shows the reduction of the total drag, which includes wave and pressure drags. The horizontal axis is the rate of air ejection in terms of the air layer thickness t_a

$$t_a \equiv \frac{Q_a}{B_a U_\infty} \quad (\text{mm}) \quad (1)$$

where Q_a is the rate of air ejection, B_a is the width of the ejection plate, and U_∞ is the ship speed.

Figure 11(b) shows the reduction of the frictional drag of the part directly downstream of the air ejection plate. This plot has been obtained by assuming that the reduction of total drag shown in Figure 11(a) was attributed to the reduction of the frictional drag component R_f , the frictional drag of the area downstream of the air injection plate. R_{f0} , the value of R_f in the non-bubble condition, was estimated using Schoenherr's formula. It is seen that the reduction at 5m/s reaches about 30%. In the same figure, the corresponding data by Watanabe et al. of IHI (1999) using a 40m-long flat plate ship and a porous plate (PP) for air ejection is plotted. The reduction in their experiment using PP is greater than that of NMRI using AHP.



(a) Total drag

(b) Frictional drag of the part covered with bubbles

Fig.11 Microbubble drag reduction of a 50m long flat plate ship at NMRI (Array of Holes Plate) (Kodama et al 2002a)

Figure 12 shows the streamwise distribution of the local skin friction reduction measured at NMRI and IHI. The horizontal axis shows the streamwise distance from the air ejection point. It is seen that the skin friction reduction persists almost to the downstream end. It is also seen that the reduction using PP is greater than that using AHP, which is consistent with the result shown in Figure 11(b).

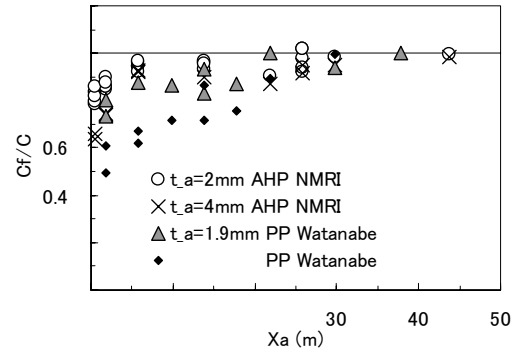


Fig.12 Comparison of the local skin friction reduction using AHP (NMRI) and PP(IHI)

Questions:

1. What is the mechanism of frictional resistance reduction by microbubbles?
2. What is the best condition of microbubbles for reducing frictional resistance?
3. How do we realize the best condition of microbubbles?

The first proposed mechanism is the decrease of turbulence intensity in the flow due to the increase of effective viscosity caused by microbubbles (Madavan et al. (1985B)). In order for this to be true, the size of bubbles should be much smaller than the turbulence scale of the flow. Gore and Crowe (1988) presented a diagram on the solid-liquid as well as solid-gas two-phase flow. According to the diagram, the size of solid particles should be one order smaller than the turbulence scale. In the experiments at NMRI and Toyo University, the height of the test section was 10 or 15mm, which corresponds to a few thousand wall units. If we assume that the governing turbulence scale is one-tenth the test section height, the size of microbubbles should be less than 0.1mm, which corresponds to 30-60 wall units. But, in reality, the bubble size was much larger than that.

Kato et al. (1999) suggested a mechanism in which a group of bubbles can be more effective than separate single bubbles in reducing turbulence intensity, even if the bubbles are larger than those shown by Gore and Crowe. Their suggested mechanism also explains a tendency that a small amount of microbubbles sometimes increases frictional resistance.

Recently Sugiyama et al. (2002) presented another explanation, which suggests that flattened bubbles near the solid wall realize a quasi-slip flow at the wall surface.

Recent measurements of the turbulence characteristics in the channel flow with microbubbles, carried out at the NMRI, are very suggestive. According to the PIV as well as PTV measurements, the turbulence intensity, such as u' and v' , was increased by microbubbles, whereas the Reynolds stress was decreased. This means that the turbulent flow becomes more isotropic with microbubbles. This tendency resembles turbulence generation behind solid spheres.

Another recent measurement of the turbulence characteristics was performed using LDV in the water channel at Toyo University. Figure 13 shows the relation of turbulence intensity and the mean void ratio. The ordinate of the figure is T/T_0 , where $T (\equiv \sqrt{u'^2} / u)$ and T_0 are turbulence intensities with and without microbubbles, respectively. The parameter y is the distance from wall, which was estimated from the measured mean velocity profile. The turbulence intensity decreased with the mean void ratio in the region very close to the wall ($y \leq 0.025\text{mm}$). In contrast, the turbulence intensity in the outer region increased with the mean void ratio. The distance of 0.025mm corresponds to 10-15 wall units. The result needs caution, because the diameter of the laser beam was about 0.1mm. We need further verification on the LDV measurement. This data can be directly compared with that by the PIV/PTV techniques taken at NMRI, because the water channel of Toyo University (100mm x 10mm cross section) is similar to that of NMRI (100mm x 15mm cross section).

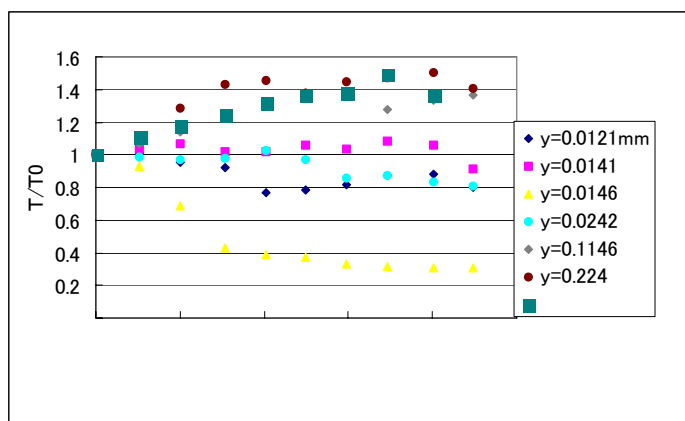


Fig. 13 Change of turbulence intensity with mean void fraction (y: distance from wall)

To summarize, there are possibly two different mechanisms for frictional resistance reduction by microbubbles. One is the reduction of turbulence intensity due to the increase of apparent viscosity caused by the bubbles less than 0.1mm in diameter. In other words, a kind of relaminarization arises. The other is the mixing for homogenization by microbubbles larger than the turbulence scale. We usually observe this mechanism in the model as well as full-scale experiments.

We should examine whether the two mechanisms are true, or whether there is a third mechanism, such as slip at the wall suggested by Sugiyama et al.

The second and third questions on how to realize a microbubble distribution optimum in bubble size and bubble number density are also very important for the practical application of microbubbles.

5. Concluding Remarks

We introduced the recent research work by the SR 239 Research Committee: (1) full-scale microbubble experiment of the Seiun-Maru, and (2) air sheet experiment. These are very instructive and provide important suggestions and lessons for the practical application of air-based skin friction reduction devices. We have suggested two possible mechanisms of frictional resistance reduction by microbubbles.

In our group, young colleagues are eagerly, and sometimes sleeplessly, studying the mechanism using numerical simulation techniques or frontier experimental techniques, and have obtained many interesting findings. In this presentation we did not touch upon their findings, because they are cleverer than us and will make better presentations on their achievements.

References

- Bogdevich V. G., Evseev A. R., Malyuga A. G. et al.,1977, Gas saturation effect on near-wall turbulence characteristics. Second International Conference on Drag Reduction, Cambridge, England, BHRA, 25-37
- Gore R. A., Crowe C. T., 1988, Effect of particle size on modulating turbulent intensity. *J Multiphase Flow* Vol.15, No.2, 279-285
- Guin M. M., Kato H., Yamaguchi, H. et al., 1996, Reduction of skin friction by microbubbles and its relation with near-wall bubble concentration in a channel. *J Mar Sci Technol*, 1, 241-254
- Kato, H., Iwashina, T., Miyanaga, M., Yamaguchi, H. et al., 1999, Effect of microbubbles cluster on turbulent flow structure. IUTAM Symposium on Mechanics of Passive and Active Flow Control, 255-260
- Kato, H., Ikemoto, A., Toda, Y., 2003, Void fraction measurement in the boundary layer of training

- ship Seiun-Marun, Symposium on Microbubble and Polymer Friction Drag Reduction, ASME-JSME FED-SM 2003.
- Kodama, Y. et al., 2002a, Microbubbles: Drag Reduction Mechanism and Applicability to Ships, 24th Symposium on Naval Hydrodynamics, Fukuoka, JAPAN, July 2002.
- Kodama, Y. et al., 2002b, A full-scale experiment on microbubbles for skin friction reduction using Seiun-Marun, Part 1: The preparatory study, J Soc of Naval Architects of Japan, 192,1-13 (in Japanese)
- Kodama, Y., 2002, Possibility and tasks for the practical application of microbubbles, Symposium on the Turbulent Flow Research and Its Applications, JTTC Symposium, SNAJ.150-185 (in Japanese)
- Madavan, N. K., Deutsch, S., Merkle, C. L., 1985A, Measurements of local skin friction in a microbubble-modified turbulent boundary layer. J Fluid Mech, 156, 237-256
- Madavan, N. K., Merkle, C. L., Deutsch, S., 1985B, Numerical investigations into the Mechanisms of microbubble drag reduction, J Fluids Eng., Trans. ASME, 107, 370-377
- Moriguchi, Y., Kato, H., 2002, Influence of microbubble diameter and distribution on frictional resistance reduction. J Mar Sci Technol, 7, 79-85
- Nagamatsu, T. et al., 2002, A full-scale experiment on microbubbles for skin friction reduction using Seiun-Marun, Part 2: The full-scale experiment, J Soc of Naval Architects of Japan, 192,15-28 (in Japanese)
- Shimoyama, N., 2002, Reduction of frictional resistance of ships by air-sheet method, Symposium on the Turbulent Flow Research and Its Applications, JTTC Symposium, SNAJ.186-209 (in Japanese)
- Sugiyama, K. et al., 2002, Numerical simulations on drag reduction mechanism by microbubbles, 3rd Symposium on Smart Control of Turbulence, University of Tokyo, Tokyo.
- Takahashi, T. et al., 2001, Mechanisms and scale effects of skin friction reduction by microbubbles, 2nd Symposium on Smart Control of Turbulence, University of Tokyo, Tokyo.
- Watanabe. O., Masuko. A., Shirase, Y., 1999, Measurements of drag reduction by microbubbles using a very long ship models. J Soc of Naval Architects of Japan, 183, 53-63 (in Japanese)